Temperature Dependence of Triplet-Exciton Dynamics in Anthracene Crystals

V. Ern,* A. Suna, Y. Tomkiewicz, P. Avakian, and R. P. Groff

Central Research Department,† E. I. du Pont de Nemours & Company, Wilmington, Delaware 19898

(Received 30 August 1971)

The component of the triplet-exciton diffusion along the crystal a axis was measured in anthracene crystals at 118, 160, 298, and 371 °K, and found to be $D_{aa} = (4.0 \pm 0.5)$, (2.5 ± 0.3), (1.5 ± 0.2), and $(1.6 \pm 0.3) \times 10^{-4}$ cm^2 sec^{-1}, respectively. The polarized-excitation spectra (0, 0 line) for delayed fluorescence have also been measured. The inferred values for the Davydov splitting Δ and the effective scattering rate Γ at the corresponding temperatures are $\Delta = 18 \pm 2$, 18 ± 6, 17 ± 3, and 19 ± 2 cm^{-1} and $\Gamma = 14 \pm 1$, 30 ± 2, 51 ± 1, and 65 ± 2 cm^{-1}. The simultaneous measurement of these parameters, in conjunction with an expression for diffusion derived from a phenomenological model of triplet-exciton scattering, allows the assessment of the relative importance of local vs nonlocal scattering mechanisms in the triplet-exciton motion. The nonlocal scattering rate, due to fluctuations in the exciton-transfer matrix elements between molecules separated by $\pm \frac{1}{2}(a \pm b)$, is estimated to be ~ 0.1 cm^{-1}, and appears to be temperature insensitive. The local scattering mechanism is dominant, but the nonlocal fluctuation rates can make a sizable contribution to the rate of triplet transport. The spectroscopic measurements show that the hopping model for transport is applicable in the temperature range studied.

I. INTRODUCTION

The room-temperature value of the diffusion constant for triplet excitons in anthracene is well known.[1-3] Additional information on triplet-exciton dynamics can be obtained from spectroscopic data,[4] which lead to the conclusion that at room temperature triplet excitons in anthracene move by a hopping process; the spectroscopic information also yields an estimate of the diffusion constant, provided one admits certain simplifying assumptions. Assuming absence of self-trapping, local exciton scattering, and a Lorentzian line shape, the authors of Ref. 4 obtained an estimate of 0.5×10^{-4} cm^{2}sec^{-1} for D_{aa}, the component of the diffusion tensor along the $\vec{a}$ crystal axis. In view of the uncertainties in this estimate it compares well with the directly measured value[2] of 1.5×10^{-4} cm^{2}sec^{-1}.

This spectroscopic approach to exciton dynamics has been used by Durocher and Williams[5] to investigate triplet excitons in anthracene for a range of temperatures; more recently, the method has been also applied to study exciton dynamics in other systems.[6] A comparison of the spectroscopically estimated values of the diffusion constant with directly measured ones provides a test of the assumptions of the spectroscopic method. For anthracene, direct measurements of D_{aa} for temperatures other than room temperature have not been reported before the present paper. The value of the diffusion constant near liquid-nitrogen temperature has, however, been inferred from determinations of the spin relaxation times of triplet excitons[7] as well as from the measured influence of triplet excitons on proton spin relaxation times.[8,9] Both sets of experiments[7,9]

have been interpreted so as to imply about a 30% increase of D at the lower temperature, compared to D at room temperature as obtained by the same techniques. These results sharply contradict the spectroscopic estimate of Ref. 5, which predicts a ratio $D_{aa}(130 °K)/D_{aa}(300 °K) \approx 6$.

Perhaps the most sensitive assumptions[4] involved in the spectroscopic estimate of the diffusion constant were the assumption of absence of self-trapping and the assumption of local scattering of excitons. Further support for the absence of self-trapping, in the form of an undetectable (within ± 5 cm^{-1}) Stokes shift of the 0, 0 line of the phosphorescence emission above 55 °K, has recently been given by Goode and Williams.[10] In this paper, we wish to reexamine the assumption of purely local exciton scattering. Nonlocal scattering of excitons, arising from fluctuations in the exciton-transfer matrix elements, has been included by Haken and Strobl[11] in their theory of exciton motion. Recently, Grover and Silbey[12] have argued that for strong coupling of excitons and phonons, the nonlocal scattering is dominant, and have presented a theory of the temperature dependence of the diffusion constant based entirely on nonlocal scattering. A weak-coupling theory, on the other hand, can give rise to local scattering.[13] An experimental resolution of the question of the relative importance of local versus nonlocal scattering of triplet excitons in anthracene thus appears to be of considerable interest.

In the present study, we report direct measurements of D_{aa} for triplets in anthracene at various temperatures, together with temperature-dependent spectroscopic measurements of the delayed-fluorescence polarized excitation spectra of the 0, 0

line of the lowest anthracene triplet state. We also verify phosphorescence emission spectra (0, 0 line) reported previously.[10] We present a theoretical discussion of the model of nonlocal scattering introduced in Ref. 11 and derive an exact expression for the diffusion tensor for this model. The expression for D_{aa} involves essentially three phenomenological parameters, a total scattering rate Γ, the Davydov splitting Δ, and γ_d, the fluctuation rate of the exciton-transfer matrix elements between molecules separated by $\pm \frac{1}{2}(\vec{a} \pm \vec{b})$. The effective value of Γ is obtained with the aid of the hopping-model formula of Dexter[14] and of Trlifaj,[15] using the absorption spectra derived from the measured excitation spectra. The splitting Δ is computed as the difference in mean energies, calculated as centroids[16] of the a- and b-polarized absorption spectra. The theoretical expression for the diffusion constant together with the measured value and the known parameters Δ and Γ then enables us to deduce a value of γ_d for each temperature. Finally, we present a discussion of the apparent contradictions between existing magnetic-resonance results[7,9] and the present experiments.

II. THEORETICAL BACKGROUND

A. Phenomenological Model for Exciton Motion

A phenomenological model of exciton scattering, useful in analyzing exciton dynamics at temperatures such that kT is large compared to the exciton bandwidth, has been recently presented by Haken and Strobl.[11] The model treats the exciton Hamiltonian as consisting of the sum of an average, or time-independent, part $\mathcal{H}$ and a time-varying part $h(t)$, which is treated phenomenologically. The matrix elements $h_{nm}(t)$ in a spatial representation (excitons localized at $\vec{R}_n$ or $\vec{R}_m$) are assumed to have the following property:

$$\langle h_{nm}(t+\tau) h_{n'm'}(t) \rangle = [\delta_{nn'}\delta_{mm'} + \delta_{nm'}\delta_{mn'}(1-\delta_{nm})]$$
$$\times 2\gamma_{m-n}\delta(\tau) , \quad (1)$$

where $\langle \rangle$ denotes an average over t, and where the parameters γ_{m-n} are understood to be functions of $\vec{R}_m - \vec{R}_n$. Furthermore, it is assumed that averages of higher products of h_{nm}'s can be expanded in terms of (1), i.e., that the cumulant averages[17] of a product of more than two h_{nm}'s all vanish. With these assumptions, the equation of motion of the exciton density matrix ρ takes the form ($\hbar = 1$)

$$(\partial/\partial t)\rho_{nm} = -i[\mathcal{H}, \rho]_{nm} - 2(\textstyle\sum_l \gamma_l)\rho_{nm} + 2\delta_{nm}\textstyle\sum_l \gamma_{n-l}\rho_{ll}$$
$$+ 2(1-\delta_{nm})\gamma_{n-m}\rho_{mn} . \quad (2)$$

The same equation of motion was used in Ref. 4, where, however, only the local scattering term γ_0 was assumed to be nonvanishing. It was argued in Ref. 4 that nonlocal scattering should be equivalent

to wave-vector-dependent scattering and should therefore manifest itself by producing a different line shape for the two Davydov components in a polarized light absorption experiment. The observation of nearly identical line shapes for the two components at room temperature then supported the neglect of nonlocal scattering terms. It can be shown, however, that a wave-vector-independent exciton scattering results when the fluctuations of the transfer matrix element between a given pair of molecules is uncorrelated with that for any other distinct pair, as assumed in Eq. (1). As shown in Appendix A, Eq. (1) implies a Lorentzian absorption line shape of the same half-width,

$$\Gamma \equiv \textstyle\sum_l \gamma_l , \quad (3)$$

for both Davydov components. Although the noncorrelation assumption on the transfer matrix elements is clearly incorrect for scattering due to acoustic phonons (the motion of a given molecule simultaneously affects the transfer matrix elements to all of its neighbors), Grover and Silbey[12] have argued that such predominantly uncorrelated scattering can arise from interactions with internal vibrations of the molecules since, for strong coupling with such vibrations, exciton-transfer matrix elements contain a Franck-Condon factor[18] which undergoes thermal fluctuations at finite temperatures.

Insofar, then, as the assumptions implicit in (1) are applicable to excitons in a real molecular crystal, it is of interest to investigate the implications of (2) on measurements of exciton diffusion. As shown in detail in Appendix B, and as is expected on general grounds in a dissipative system,[19] Eq. (2) reduces to a diffusion equation in the limit of large times and long wavelengths for the spatial exciton density.[20] The diffusion tensor is given by

$$D_{\mu\nu} = \textstyle\sum_{\vec{R}} R_\mu R_\nu [\gamma_{\vec{R}} + \tfrac{1}{2}\beta_{\vec{R}}^2/(\Gamma + \gamma_{\vec{R}})] , \quad (4)$$

where $\beta_{\vec{R}}$ is the transfer matrix element for transfer between a molecule at, say, $\vec{R}_0$ and one at $\vec{R} + \vec{R}_0$. The sum extends over all lattice vectors, but for triplet excitons it is expected to be accurately approximated by considering nearest-neighbor $\vec{R}$'s only.

Expression (4) differs from the corresponding expression of Ref. 1 in that the quantities $\gamma_{\vec{R}}$ ($\vec{R} \neq 0$) are present, both explicitly and implicitly in the total scattering rate Γ [Eq. (3)]. If these quantities are not negligible compared to both γ_0 (and hence to Γ) and $\frac{1}{2}\beta_{\vec{R}}^2/\Gamma$, the knowledge of the half-width of the Lorentzian absorption spectrum and of the transfer matrix elements $\beta_{\vec{R}}$ is not sufficient for inferring the exciton diffusion tensor. Equation (4) can be used to obtain information on the $\gamma_{\vec{R}}$'s if measurements of the exciton diffusion tensor are made.

B. General Line Shapes, Hopping Model

A potential difficulty in applying the phenomenological expression (4) to real systems is that a Lorentzian spectral shape is required. A formula for the diffusion tensor which does not have this difficulty is the hopping-model formula obtained by Trlifaj,[15] following Dexter's theory[14] of energy transfer in doped systems. In the hopping model one has

$$D_{\mu\nu} = \tfrac{1}{2} \sum_{\vec{R}} R_\mu R_\nu \Psi(\vec{R}) , \qquad (5)$$

where $\Psi(\vec{R})$ is the exciton hopping rate between two molecules separated by $\vec{R}$. Trlifaj's formula is[21,22]

$$\Psi(\vec{R}) = \beta_{\vec{R}}^2 \, 2\pi \int_{-\infty}^{\infty} d\omega f(\omega) F(\omega) , \qquad (6)$$

where $f(\omega)$ and $F(\omega)$ are, respectively, the normalized emission and absorption spectra, which can be arbitrary functions of the photon frequency ω. Application of (6) to the coincident Lorentzian absorption and emission spectra implied by (1) yields

$$\Psi(\vec{R}) = \beta_{\vec{R}}^2 / \Gamma , \qquad (7)$$

whereas expression (4) implies a jump rate

$$\Psi(\vec{R}) = 2\gamma_{\vec{R}} + \beta_{\vec{R}}^2 / (\Gamma + \gamma_{\vec{R}}) . \qquad (8)$$

The inconsistency between (7) and (8) arises because Trlifaj[15] in his derivation assumes that exciton-transfer terms in the Hamiltonian are independent of the positions of the molecules; thus there is no possibility of fluctuations of these transfer terms.

Formulas (4) and (5) with (6) are in some ways complementary. Although limited to Lorentzian spectra, formula (4) is not restricted to the hopping model but is applicable to partially coherent exciton motion as well; it is, however, limited to temperatures large compared to the exciton bandwidth, since the theory leading to this expression implies a uniform population of all exciton states at equilibrium [the steady-state solution of (2) is $\rho_{nm} = N^{-1} \delta_{nm}$]. Formula (6), on the other hand, works whenever the hopping model is applicable and when nonlocal scattering can be neglected, regardless of the temperature and of the shape of the spectra.

For molecular crystals, spectra frequently consist of a series of vibronic peaks, of which the main progression has an energy spacing large compared to kT for all reasonable temperatures. As a result, since thermal relaxation between the vibronic states is fast compared to triplet decay rates, exciton dynamics involves only the lowest vibronic band of this progression, characterized by properties of the 0, 0 peak.[1] Formula (6) gives the correct hopping rate in this case even if the range of ω is restricted to the region of the overlapping 0, 0 peaks in emission and absorption, provided the quantity $\beta_{\vec{R}}$ is understood to be the transfer matrix element for the exciton in its lowest vibronic state

($\beta_{\vec{R}} = C_{0,0} \beta_{\vec{R}}^{\text{tot}}$, where $C_{0,0}$ is the Franck-Condon factor for the 0, 0 transition[18]).

Even if only the 0, 0 peak is retained in the spectra, this peak may still not have a line shape which is sufficiently close to a Lorentzian to allow an unambiguous assignment to the parameter Γ of the phenomenological theory. Although a rigorous generalization of this theory, so as to apply to arbitrary line shapes, is not available, it is reasonable to define an effective Γ by the relation

$$\Gamma = [2\pi \int_{0, 0 \text{ peak}} d\omega f(\omega) F(\omega)]^{-1} . \qquad (9)$$

This relation is an identity for the case of coincident Lorentzian absorption and emission spectra of half-width Γ, and one will, at least, be assured of obtaining the correct answer for the diffusion constant from Eq. (4) when nonlocal scattering is negligible and when the hopping model is applicable. Note that the integral must be restricted to the region of the 0, 0 peak and that the transfer matrix elements $\beta_{\vec{R}}$ in Eq. (4) are those for the exciton in its lowest vibronic state.

By defining Γ via (9) and assuming Eq. (4) to be applicable one can always find quantities $\gamma_{\vec{R}}$ so as to yield experimentally measured values of the diffusion constant. The exact interpretation of these quantities as fluctuation rates of the corresponding matrix elements [Eq. (1)] may not be clear cut if the deviation from a Lorentzian line shape is large. Even in this case, as long as setting $\gamma_{\vec{R}} = 0$ is inconsistent with the measurements and the hopping model is applicable, one can at least say that some form of nonlocal scattering must be present in the exciton motion.

III. EXPERIMENTAL

The experimental setup for the measurements of the singlet-triplet ($T_1 \leftarrow S_0$) excitation spectra for delayed fluorescence was a modification of the apparatus reported earlier.[4] Light, from a 1000-W xenon arc lamp (Hanovia 976C-1), was filtered through 10 cm of water and a red-transmitting blue-cutoff filter (Schott No. OG-1), 3 mm thick), dispersed via a monochromator (Spex model 1700 with a Bausch & Lomb 1200-grooves-per-mm grating blazed at 7500 Å, with a dispersion of 10.5 Å per mm in the spectral range of interest), and relayed via lenses and a polarizing filter (Klinger Scientific No. 036320 with an Erwin Käsemann Ks DEM-W-58 polarizer) onto the crystal. The delayed fluorescence from the crystal was led with a Pyrex light guide to a photomultiplier (EMI 6255-SA) through a blue-transmitting red-absorbing filter stack (Corning C. S. 4-76 and C. S. 7-59 filters and an Optics Technology broad-band interference filter with 50% transmission points at 3700 and 4525 Å, or Corning C. S. 4-72 + 5-58 filters; for measurements above

room temperature one C. S. 4-72 and three C. S. 5-60 Corning filters were used). The photomultiplier output was fed via an operational amplifier to an integrator (Technical Measurements Corp. CAT Model 400) or to a strip-chart recorder. In measurements above room temperature, where a higher intensity was needed, a wider-slit monochromator (Bausch & Lomb, 500-mm grating with 16.5-Å-per-mm dispersion) was used. The monochromators were provided with a synchronous-motor wavelength-drive mechanism with a microswitch for triggering the CAT. Wavelength-drive rates between 25 and 100 Å min⁻¹ were used. The CAT was operated in the external address advance mode, using a crystal-controlled pulse generator, at a rate of 0.4 sec per channel (160-sec full sweep for the 400 channels). To achieve adequate signal-to-noise enhancement, up to several dozen CAT scans were employed. A low-pressure argon lamp (Pen-Ray Ultra-Violet Products) was used for wavelength calibration.

In the low-temperature measurements the crystals were placed in a glass cryostat with optical windows at its bottom and cooled with a flow of nitrogen gas. The temperature was measured with a copper-constantan thermocouple in contact with the sample. A second thermocouple monitored the temperature of the chamber near the sample. In measurements above room temperature the samples were surrounded by a heater capped with a glass Dewar. At any given temperature the sample and its holder could be rotated in order to control the orientation of the crystal axes with respect to the electric vector $\vec{E}$ of the incident light beam.

The crystals, typically 2–3 mm thick, were cleaved along the ab plane from ingots grown from the melt of highly purified[23] anthracene. Triplet lifetimes were about 20 msec. The incident light was perpendicular to the ab plane and had a cone of incidence of ~20°. The polarization ratio (the ratio of delayed-fluorescence intensity with $\vec{E} \| \vec{a}$ to that with $\vec{E} \| \vec{b}$) was measured at room temperatures by setting the incident wavelength at 6779 Å (the average position of the two Davydov components) and recording the emitted delayed-fluorescence intensity as the crystal was rotated with respect to the $\vec{E}$ vector. At −184 °C the Davydov components appear sufficiently separated and the polarization ratio was obtained by comparing the peak intensities in the two components. It was ascertained that the effect of slit width on the spectral line shape was negligible.

The direct measurements of triplet-exciton diffusion lengths were performed with the delayed-fluorescence phase-detecting technique described earlier.[2] The ab-plane anthracene platelets were cooled and heated by a technique similar to the one used for the spectroscopic measurements. The

spatially nonuniform triplet-exciton distributions in the crystal were produced with 1:1 images of Ronchi rulings placed outside the cryostat at the appropriate position in the optical path of the beam of the He-Ne laser. The spatial periodicity of the exciting light intensity distribution in the plane of the samples was verified with a microscope and by regularly checking the induced changes in the phase of delayed fluorescence against those obtained by placing the rulings directly below the crystal. This optical arrangement considerably simplified the experiments, allowing, at a given temperature, a complete scan of the dependence of the phase lag of delayed fluorescence on the spatial distribution of the intensity of the exciting light. For all samples nearly negligible levels ($\Delta i/i_0 = 3-5\%$) of stray light correction in the shadow regions were needed for best fit of the data to the predicted behavior for the phase of the delayed fluorescence.[2]

The expressions relating the phase lag of delayed fluorescence to the triplet lifetime τ, to the diffusion length L_α along a given direction α in the plane of the sample, and to the spatial period x_0 of the exciting light have been given in Ref. 2. From the diffusion length, defined in the usual manner $[L_\alpha \equiv (2D_\alpha \tau)^{1/2}]$, one obtains D_α, the magnitude of the exciton diffusion tensor in a given direction. The triplet-exciton lifetime at each temperature was obtained from the phase lag of delayed fluorescence under uniform excitation of the sample (e.g., $L_\alpha/x_0 \ll 1$ in Ref. 2). In several runs the deduced lifetimes were also verified by accumulating the waveforms in a computer of average transients, and the triplet lifetimes were deduced from the exponential decay of the delayed fluorescence. For the samples studied the lifetimes were nearly constant ($\tau \approx 18-20$ msec) in the 200–400 °K range and decreased by nearly a factor of 2 ($\tau \approx 10-20$ msec) after cooling to 118 °K. A similar behavior of lifetime has been recently reported by Arnold $et~al.$[24] for high-purity unstrained anthracene crystals.

Measurements of triplet-exciton diffusion along the crystal a axis were performed at 118, 160, 298, and 371 °K. The results are $D_{aa} = (4.0 \pm 0.5)$, (2.5 ± 0.3), (1.5 ± 0.2), and $(1.6 \pm 0.3) \times 10^{-4}$ cm²sec⁻¹, respectively. The corresponding 0, 0 lines of the delayed-fluorescence excitation spectra, after corrections as explained in Sec. IV, are displayed in Fig. 1.

IV. INTERPRETATION OF EXPERIMENTS

A. Davydov Splittings

Merrifield[16] has shown that the proper way to determine the Davydov splittings of complex spectra is to calculate the differences in mean energies calculated as the centroids of the absorption spectra of the various components. For an absorption
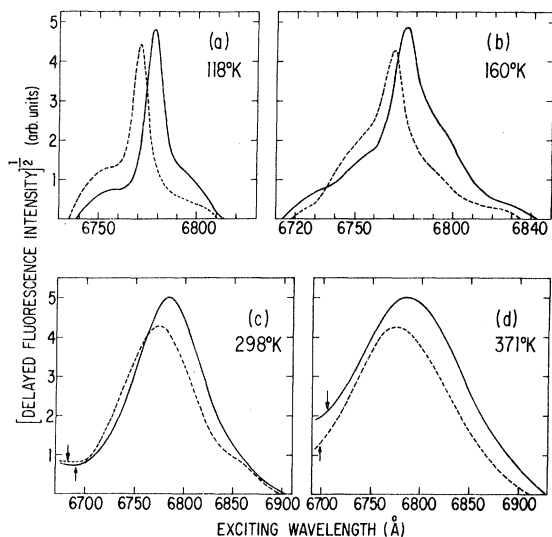
FIG. 1. First band (0, 0 line) of the polarized excitation spectra for triplets in anthracene crystals at (a) 118, (b) 160, (c) 298, and (d) 371 °K. The quantity plotted is the square root of the measured delayed-fluorescence intensity $\Phi^{1/2}$. The full curves are for $\vec{E} \parallel \vec{a}$ crystal axis. The dashed curves are for $\vec{E} \parallel \vec{b}$ crystal axis after correction for the presence of the mainly a-polarized component as explained in text. The arrows in (c) and (d) indicate the assumed cutoffs for calculating $\overline{\omega}$ and Γ [Eqs. (10) and (12) in text]. The vertical scales are arbitrary, and do not reflect the actual relative heights of the a and the b components. Note the change in horizontal scale for (c) and (d).

spectrum given by the square root of the delayed-fluorescence excitation spectrum $\Phi(\omega)$ as a function of the photon frequency ω, the mean value $\overline{\omega}$ is given by

$$\overline{\omega} = \int d\omega\, \omega[\Phi(\omega)]^{1/2} / \int d\omega'[\Phi(\omega')]^{1/2} . \qquad (10)$$

This equation can be applied not only to the complete spectra (for all frequencies) when the full electronic Davydov splitting is obtained from the mean-energy differences of the two components, but also for each vibronic component of the full spectrum. The result is then the splitting of that particular component, equal to the full splitting times an appropriate Franck-Condon factor.[18] In the latter case, applicable to the present experiments, it is, of course, necessary that the vibronic components can be resolved from one another. This technique will yield the same result for the splitting as that obtained from the difference in peak positions if the spectra of both Davydov components (i.e., a- and b-polarized spectra for anthracene) have the same shape. This is not the case for excitation spectra in anthracene, where asymmetries which are different for the a and b components have been reported,[5] and as is particularly evident in Fig. 1(b). Al-

though the differences in the spectra of the two components are small, the Davydov splitting is also small in comparison to the total linewidth except at the lowest temperatures, so that splittings obtained by differences in peak positions can be grossly incorrect.

In computing Davydov splittings via (10), it is important that the b-polarized spectrum (giving mainly the "minus" Davydov component)[25] be corrected for the contribution of the (mainly a-polarized) "plus" component, which is more intense and seems always to be present in experiments in amounts depending on the particular experimental setup and the crystal used. In the setup for the three lowest temperatures given in Table I, the b-polarized spectrum obtained at 90 °K allowed resolution of the "plus" peak, whose magnitude in absorption was about 0.16 that of the "minus" peak. Another way of estimating this contribution is by comparing high-temperature polarization ratios with the theoretical value[25] of 3.62 (which we verified experimentally at 90 °K), where the polarization ratio is measured at a wavelength midway between the two components. The ratio is reduced to 3.62/ $(1 + x)$, where x is the fraction of the "plus" component in the b-polarized spectrum. This procedure gave $x = 0.17$ at room temperature, consistent with the above. For the high-temperature setup, where x could only be deduced from the polarization ratio, we found $x = 0.8$. Some reasons for the presence of the "plus" component in the b-polarized absorption spectrum are (a) the theoretical expectation[25] that b-polarized light is absorbed to some extent by the primarily a-polarized "plus" Davydov component, the ratio of "plus" to "minus" absorption being about 0.02, (b) crystal imperfection effects causing misalignments and depolarization of the

TABLE I. Summary of measured and calculated parameters.

	Temperature (°K)			
	118	160	298	371
D_{aa} $(10^{-4}\,cm^2\,sec^{-1})$	4.0 ± 0.5	2.5 ± 0.3	1.5 ± 0.2	1.6 ± 0.3
Δ (cm^{-1})[a]	18 ± 2	18 ± 6	17 ± 3	19 ± 2
Γ^b (cm^{-1})[a]	14 ± 1	30 ± 2	51 ± 1	65 ± 2
Γ^c (cm^{-1})[a]	14 ± 2	26 ± 6	54 ± 6	62 ± 2
$a^2\Delta^2/64\Gamma$ $(10^{-4}\,cm^2\,sec^{-1})$	$2.5^{+0.8}_{-0.6}$	$1.1^{+1.0}_{-0.6}$	0.6 ± 0.2	0.6 ± 0.1
γ_d (cm^{-1})[a]	$0.11^{+0.09}_{-0.08}$	$0.10^{+0.10}_{-0.06}$	0.07 ± 0.04	0.07 ± 0.03

[a]The equivalent rates (sec^{-1}) are obtained by multiplying by $2\pi c \approx 1.88 \times 10^{11}$ cm sec^{-1}.
[b]From the a-polarized component.
[c]From the b-polarized component.

exciting light by scattering, and (c) the fact that, in the present experiments at least, the light incident on the crystal was partially focused, with the resulting deviations from normal incidence introducing a c^* component in the $\vec{E}$ vector of the incident light, which couples strongly to the "plus" Davydov component.[25]

A difficulty present only in the high-temperature spectra is that the 0, 0 peak is not perfectly resolved [e.g., Fig. 1(c)] from the next vibronic peak. We have adopted the procedure, illustrated by the arrow in Fig. 1(c), of cutting off the spectra near the flat minimum separating the 0, 0 peak from the next vibronic peak. Obviously, the precise choice of the cutoff point affects the position of the calculated mean energy. We have chosen the cutoff points such that for both components the distance between peak maximum and cutoff is the same. This choice ought to minimize the error in the Davydov splitting introduced by the cutoff, since for the case of identical line shapes of both components only this choice of cutoff avoids introducing an artificial error in the splitting.

A further source of error was present in the analysis of the 371 °K spectra, where the delayed-fluorescence emission was superimposed on a low background of prompt emission, apparently due to direct absorption in the singlet tail. The magnitude and wavelength dependence of this background were deduced by comparing spectra for different slit widths and using the fact that delayed-fluorescence intensity varies as the square of the incident intensity, while prompt fluorescence is linear in intensity. Since singlet absorption in the Urbach tail is also strongly polarized.[26] the background correction was quite different for the a- and b-polarized spectra. Therefore, any errors in this correction lead to an error in the splitting.

The calculation of the splitting from the mean energies has the additional advantage that all the experimental points are used, with a resulting reduction in the experimental error. A careful estimate of the errors in the splitting is essential, since these give by far the greatest contribution to the errors in the spectroscopic estimates of the diffusion constant. We have estimated the rms error in the position $\bar{\omega}$ of the centroid by the formula

$$\langle(\delta\omega)^2\rangle^{1/2} \approx \frac{\pi^{-1}(\frac{1}{14}\xi\eta)^{1/2}(\eta/\Gamma)^3\epsilon}{\Phi(0)} , \tag{11}$$

derived under the assumptions stated in Appendix C. In Eq. (11), ξ is the resolution for a CAT channel, 2η the full spectral range, Γ the half-width of the equivalent Lorentzian, ϵ the rms noise amplitude, and $\Phi(0)$ the value of the signal at the peak. No attempt has been made to estimate the uncertainties introduced by the cutoff and the background

subtraction used for the high-temperature spectra.

The numerically computed Davydov splittings for the spectra shown in Fig. 1 are given in Table I, where the listed errors are calculated with the aid of (11). Similar procedures applied to spectra at 90 and 228 °K gave Davydov splittings of $\Delta = 18 \pm 4$ and 17 ± 5 cm^{-1}, respectively. Thus, within the stated errors, the splitting appears to be temperature insensitive in the range 90–371 °K. The apparent shallow minimum[5] in the vicinity of 220 °K results if the splittings are determined from the separation of maxima of the two lines instead of the rigorous procedure[16] taking into account the complete line shapes, which near this temperature show the greatest asymmetries.

B. Effective Linewidths

The value of the effective linewidth Γ obtained by Eq. (9) will in general differ considerably from that obtained[4–6] by measuring the half-width at quarter-maximum of the observed excitation spectrum, even if this spectrum is nearly equal to the square of a Lorentzian near the peak. The reason for this can be found in the unphysical wings of a Lorentzian, which drop off so slowly (as ω^{-2}) that if they are cut off for frequencies greater than about five half-widths, the value of (9), assuming equal truncated Lorentzians for $f(\omega)$ and $F(\omega)$, is decreased to about one-half the Lorentzian half-width (the decrease is mainly due to the change in the normalization constant introduced by the cutoff). Real spectra, even if well approximatable by Lorentzians near the peak, are not expected to have wings decreasing only as ω^{-2}; the Urbach rule implies an exponential decrease, at least on the low-energy side of the absorption edge.[26] In view of this, we believe that formula (9) can be applied directly to the observed spectra without worrying about possible contributions due to essentially unobservable wings.

Emission spectra are needed in the evaluation of (9). Because of the extremely low phosphorescence intensity of anthracene, we have not been able to obtain phosphorescence spectra with the precision obtained for the excitation spectra, particularly at low temperatures. For this reason, we prefer to deduce the emission spectra from the absorption spectra using the condition of detailed balance, which essentially implies[27] $f(\omega) \propto F(\omega)\exp(-\hbar\omega/kT)$. The prerequisite for validity for this relation is that both emission and absorption occur under conditions of thermal equilibrium of the lattice. This prerequisite may be violated if there occur, during the exciton's motion, slow but important relaxation processes whose rate is slow compared to the exciton decay rate. Such a process should manifest itself in the form of a Stokes shift of the positions

of the 0, 0 peak in emission vs absorption. The evidence[10,28] is against a Stokes shift comparable to kT. Our own phosphorescence measurements[29] also showed negligible Stokes shifts in the temperature range of 298–77 °K; moreover, the observed linewidths were essentially the same as in the square root of the excitation spectra, as expected from the condition of thermal equilibrium. The effective Γ was then calculated from the observed excitation spectra $\Phi(\omega)$ by[30]

$$\Gamma = \frac{\int d\omega' [\Phi(\omega')]^{1/2} \int d\omega\, e^{-\hbar\omega/kT} [\Phi(\omega)]^{1/2}}{2\pi \int d\omega \Phi(\omega) e^{-\hbar\omega/kT}} \ . \quad (12)$$

This quantity was numerically evaluated both for the a- and corrected b-polarized spectra (Table I). Since the theory which leads to (6) implies identical line shapes for both Davydov components,[31] the discrepancy in the values of Γ computed for the two components provides a quantitative measure of the error due to the fact that the line shapes are not exactly identical. Indeed, the greatest relative discrepancy in Γ occurs for the 160 °K spectra shown in Fig. 1(b),[32] where the observed qualitative differences of the spectra of the two components was greatest.

By making an error estimate in the same way as was done for the Davydov splittings (Appendix C), we arrive at the expected errors given in Table I, which show that, in fact, the discrepancy in the values of Γ for the two components is in each case at least within experimental error. As before, no attempt has been made to estimate uncertainties such as those introduced by the cutoffs of the high-temperature data, or by possible long tails in the spectra which may be lost in the background noise.

C. Applicability of Hopping Model

The values of Δ and Γ (Table I) allow us to decide on the applicability of the hopping model of exciton motion in the temperature range investigated. The mean free path λ_a for exciton motion along the a axis is given by[4] $\lambda_a = a\Delta/16\Gamma$, so that $\lambda_a \ll a$ whenever $\Delta \ll 16\Gamma$. If the mean free path is small compared to a lattice spacing, many scattering events occur before exciton transfer from one molecule to another, and the transfer may be considered nearly incoherent.

The relation $\Delta \ll 16\Gamma$ is satisfied for all the entries in Table I. Thus we can clearly conclude that the hopping model is applicable for describing triplet-exciton migration in anthracene over the range of temperatures covered. This conclusion also gives support to the use of Eq. (9) in our analysis of the diffusion constant.

D. Diffusion and Nonlocal Scattering

The principal axes of the triplet-exciton diffusion

tensor in anthracene are[2] a, b, and c^*. Band-structure calculations[33–35] indicate that the most important triplet-exciton transfer matrix elements are β_d, β_b, and β_{d+c}, for transfer between molecules separated by lattice vectors equivalent to $\frac{1}{2}(\vec{a}+\vec{b})$, $\vec{b}$, and $\vec{c}+\frac{1}{2}(\vec{a}+\vec{b})$, respectively. Of these, β_{d+c} is much smaller than the other two and is only relevant for exciton motion out of the ab plane. The Davydov splitting is then $\Delta = 8\beta_d$. Since one expects similar relative magnitudes for the fluctuation rates of the transfer matrix elements, we assume that only γ_d, γ_b, and γ_{d+c} are nonnegligible and that γ_{d+c} is small compared to the other two. From Eq. (4) one then obtains for the principal components of the diffusion tensor

$$D_{aa} = a^2 [\gamma_d + \tfrac{1}{2}\beta_d^2(\Gamma + \gamma_d)^{-1}] \ , \quad (13a)$$

$$D_{bb} = b^2 [2\gamma_b + \gamma_d + \beta_b^2(\Gamma + \gamma_b)^{-1} + \tfrac{1}{2}\beta_d^2(\Gamma + \gamma_d)^{-1}] \ , \quad (13b)$$

$$D_{c^*c^*} = c^{*2} [4\gamma_{d+c} + 2\beta_{d+c}^2(\Gamma + \gamma_{d+c})^{-1}] \ . \quad (13c)$$

Since spectroscopic measurements yield only Γ and $\beta_d = \frac{1}{8}\Delta$, D_{aa} [Eq. (13a)] is the only component of the tensor which in conjunction with spectroscopic data provides an unambiguous determination of a nonlocal fluctuation rate (γ_d).[36,37] Equation (13a) can be rewritten as

$$D_{aa} = \frac{a^2\Delta^2}{64\Gamma} + a^2\gamma_d \left(1 - \frac{\beta_d^2}{\Gamma(\Gamma + \gamma_d)}\right), \quad (14)$$

where the first term can be evaluated from spectroscopic data and the second term represents the correction due to nonlocal scattering. Note that this term simplifies to $a^2\gamma_d$ when the hopping model is applicable $(\beta_d \ll \Gamma)$. The first term is presented in Table I using[38] $a = 8.56$ Å; from the measured values of D_{aa} one obtains the listed values of γ_d.

Because of the large estimated errors in γ_d (which may be even larger than given in Table I owing to uncertainties which have not been included in the error estimate), definitive statements concerning the temperature dependence of γ_d cannot be made. The results do imply an upper limit of ~ 0.2 cm^{-1} on the value of γ_d.[39] The results suggest that γ_d is roughly temperature independent, contrary to the expectation that scattering due to phonons must decrease as the temperature decreases, although a γ_d which is decreasing with temperature cannot be ruled out. A temperature-independent γ_d could arise if fluctuations in the transfer matrix element β_d are not due to lattice motion but are rather due to a static disorder which leads the moving exciton to "see" a fluctuating β_d. If so, future experiments might disclose a dependence of γ_d upon the degree of crystalline perfection.

The model proposed by Grover and Silbey,[12] in which nonlocal scattering (here γ_d, γ_b, and γ_{d+c}) dominates local scattering (γ_0), is inconsistent with our measurements. The linewidth [Eq. (3)] in this

model would be $\Gamma = 4\gamma_d + 2\gamma_b$; although we do not know γ_b, we certainly do not expect it to be significantly greater than γ_d,[36] and values of Γ much greater than ~1 cm^{-1} should be inconsistent with the upper limit $\gamma_d < 0.2$ cm^{-1}. By contrast even the narrowest line observed had $\Gamma \sim 14$ cm^{-1}, so that local scattering is dominant in the temperature range investigated.

V. OTHER METHODS FOR STUDYING EXCITON DYNAMICS

A. Exciton Spin Relaxation

Haarer and Wolf[7] have studied the ESR spectra of triplet excitons in anthracene at 300 and 100 °K, and have attempted to interpret the spin relaxation times T_1 and T_2 in terms of the modulation of the dipolar fine-structure interaction by the hopping of the excitons.[40] Although they obtained a room-temperature hopping rate which is consistent with the directly measured value, the reported hopping rate at 100 °K is increased by only 30% over the room-temperature rate, in sharp contradiction to both measured and spectroscopically estimated values (which show an increase of greater than 200%). The theoretical analysis of the spin relaxation mechanism, however, has several difficulties.

If the spin relaxation is only due to the motional modulation of the fine-structure part of the spin Hamiltonian of the excitons, then the relaxation rate $1/T_1$ must be proportional to the square of appropriate matrix elements of $\mathcal{H}_A - \mathcal{H}_B$, where $\mathcal{H}_A$ and $\mathcal{H}_B$ refer to the spin Hamiltonian for an exciton residing on one of the two inequivalent molecules in the anthracene unit cell. This assumption predicts no spin relaxation when all molecules are equivalent in the lattice ($\mathcal{H}_A = \mathcal{H}_B$). The observed angular dependence of T_1 on magnetic field could only be fitted with this theory by arbitrarily neglecting cross terms involving the product of a matrix element of $\mathcal{H}_A$ with a matrix element of $\mathcal{H}_B$.[7] Such a modified expression for T_1 would, however, predict spin relaxation even in a crystal with one molecule per unit cell, thus contradicting the very idea of motional modulation, since in this case there is no modulation. Similarly, it can be shown that the motional modulation theory for T_2, as given in Appendix D of Ref. 37, does not fit the observed[7] angular dependence for T_2. Instead, the authors of Ref. 7 used a formula describing the angular dependence of T_2 when the spin relaxation is caused by fluctuations in the dipolar interaction between two like spins.[41] The applicability of this formula to describe spin relaxation of a single exciton experiencing a fluctuating spin Hamiltonian is not clear.[42] It seems to us that a meaningful comparison between the directly measured exciton jump rates and the values extracted from ESR studies cannot be made until the complete mechanism for exciton spin re-

laxation is understood.

B. Exciton-Induced Proton Spin Relaxation

Maier, Haeberlen, and Wolf[8] have deduced an exciton hopping rate from studies of the magnetic field dependence of exciton-induced proton spin relaxation. More recently, Kolb and Wolf[9] have made measurements for anthracene also at liquid-nitrogen temperature and have conducted similar experiments on naphthalene. The room-temperature values for the hopping rate are consistent, in both investigations, with direct diffusion measurements. The low-temperature data, on the other hand, seem to imply a diffusion constant which is only about 30% greater than the room-temperature diffusion constant. We wish to point out some potential difficulties in the assumptions involved in the analysis of NMR data. It appears to us that taking into account the nearly two-dimensional nature of the exciton motion[2,37] modifies this analysis sufficiently so that it is no longer possible to say that present data are inconsistent with a much larger value of the low-temperature diffusion constant. The precise determination of such large triplet diffusion constants by NMR techniques unfortunately necessitates measurements at high magnetic fields, not readily available in the laboratory.

Exciton-induced proton spin relaxation results when the exciton motion modulates the interaction between the magnetic moments of the exciton and of the proton. If, as is reasonable to assume, this interaction can be neglected except when the exciton resides on the same molecule as the proton, then the proton spin relaxation rate becomes proportional[41] to a correlation function $J(\omega)$, which is the Fourier transform of the probability that if an exciton is on a given molecule at time $t = 0$, then it is still on the same molecule a time t later. Thus $J(\omega)$ contains essentially all the information on the exciton motion in the lattice. The frequency ω is given by the energy difference between the levels involved in the transition responsible for the spin relaxation.

In Refs. 8 and 9 it was assumed that $J(\omega)$ can be approximated by a Lorentzian function and that ω can be replaced by the Zeeman energy of the triplet excitons. The first of these assumptions, however, neglects important details of the triplet-exciton motion, while the second assumption is not applicable for external fields of the order of 1 kOe and less, when the zero-field Hamiltonian of the excitons can no longer be neglected. Not only will the presence of this zero-field Hamiltonian modify the exciton energy levels and spin selection rules for the transitions, but also the proton levels will be modified since the proton, too, experiences a dipolar interaction with the electron and hole comprising the exciton. A further complication at low fields is
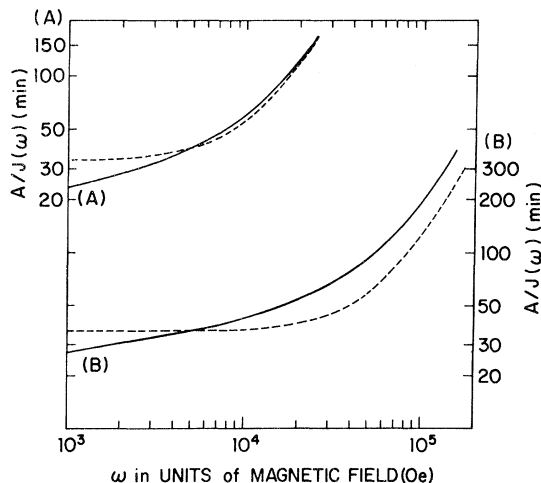
FIG. 2. Inverse of the correlation function $J(\omega)$ relevant
in the analysis of exciton-induced proton spin relaxation
in anthracene (Appendix D). The quantity plotted is
$A/J(\omega)$, with ω given in units of Oe. For fields in excess
of ~ 1 kOe the plot is equivalent to a theoretical curve for
the proton spin relaxation time T_1 appropriate for scalar
coupling (Ref. 41). The constant A has been chosen so
that for $\omega = 5$ kOe the values for T_1 are approximately
equal to the typically observed relaxation times in anthra-
cene (Refs. 8 and 9). The function has been calculated
for (A) the room-temperature triplet-exciton diffusion
tensor in anthracene (D_{aa} and D_{bb} from Ref. 2, D_{c*c*} from
Ref. 37), and (B) assuming a fivefold increase of all the
components. Corresponding curves for a Lorentzian
correlation function are shown as dashed lines.

the presence of optical spin polarization of the pro-
tons.[9,43] For purposes of studying exciton dynam-
ics, however, larger magnetic fields are sufficient;
e.g., when $D_{aa} = 1.5 \times 10^{-4}$ cm^{2}sec^{-1}, the room-tem-
perature value for anthracene, the physically im-
portant fields are in the vicinity of 12 kOe.[44]

Because of the nearly two-dimensional nature of
the motion of triplet excitons in anthracene[2,37] the
correlation function $J(\omega)$ deviates markedly from
the Lorentzian approximation $J(\omega) = \text{const}/(1+\omega^2\tau_c^2)$.
For perfectly two-dimensional motion ($D_{cc} = 0$),
$J(\omega)$ must diverge as $\omega \to 0$, since the exciton returns
to the origin infinitely often.[37,45] Correspondingly,
a nearly two-dimensional motion must have a $J(\omega)$
which is peaked near $\omega = 0$. In Appendix D, we de-
rive an exact expression for $J(\omega)$ in the hopping
model, neglecting all but nearest-neighbor transfers
of excitons. In Fig. 2, we have plotted $A/J(\omega)$,
with ω given in units of Oe and the constant A chosen
so that, for $\omega = 5000$ Oe, the value of the plotted
function is approximately equal to the typically ob-
served values of T_1 for anthracene near this tem-
perature. In this way, for fields in excess of ~ 1
kOe, the plot is equivalent to a theoretical curve
for T_1 appropriate for scalar coupling[41] of the exci-

ton and proton spin, which was used in Refs. 8 and
9. The function has been plotted for two values of
the diffusion constant, the measured room-tempera-
ture value (curve A) and a five-times-larger value
(curve B). Curves assuming Lorentzian correlation
functions for these same diffusion constants are
shown as dashed lines. The liquid-N$_2$ data of Ref.
9 do not seem to be inconsistent with curve B of
Fig. 2, or a fivefold increase of the diffusion con-
stant, although they do appear inconsistent with the
corresponding Lorentzian curve. Clearly, mea-
surements well above 10 kOe are needed for this
case if a reliable value for the diffusion constant is
to be deduced.

VI. CONCLUDING REMARKS

In the present investigation, we have endeavored
to obtain a more complete picture of triplet-exciton
dynamics in anthracene in the temperature range
118–371 °K through a combination of direct mea-
surements of the diffusion component along the
crystal a axis and spectroscopic measurements of
the Davydov splitting and effective linewidth. In
trying to assess the importance of nonlocal scatter-
ing, a detailed analysis of the spectroscopic data is
necessary. Our direct measurements of the diffu-
sion constant show that reasonable estimates of this
quantity can be made from spectroscopic data, par-
ticularly at lower temperatures. Near room tem-
perature and above, there is a definite indication
that a measure of nonlocal scattering is present in
the dynamics, though a definitive statement concern-
ing its temperature dependence could not be made.
It is clear, however, that, contrary to the model of
exciton dynamics given by Grover and Silbey,[12] the
local scattering mechanism is the dominant one,
although nonlocal fluctuation rates can contribute a
sizable amount to the exciton transport rate. Final-
ly, we can definitely conclude from the spectroscop-
ic data that the hopping model for exciton motion is
applicable for the temperature range investigated.
It is hoped that the techniques developed in the pres-
ent paper will be useful in leading to a better under-
standing of exciton dynamics in other molecular
crystals.

Note added in proof. D. Haarer informs us that
the statement in Ref. 7, that the correlation time τ_c
is only 30% shorter at 100 °K than at room tempera-
ture, is incorrect. It is the relaxation time T_2 which
is about 30% longer. This implies, using the theory
of Ref. 7, about a twofold decrease of τ_c, or about a
twofold increase of the diffusion constant over the
room-temperature value. Although this corrected
result appears consistent with the present measure-
ments, the agreement may be fortuitous in view of
the difficulties in the theoretical analysis discussed
in Sec. V.

APPENDIX A: OPTICAL LINE SHAPES

In order to derive the shapes of absorption and emission lines implied by Eq. (1) for the phenomenological exciton scattering model, it is convenient to introduce exciton creation and annihilation operators a_n and $a_n^\dagger$ for an exciton localized on $\vec{R}_n$. The time-dependent exciton Hamiltonian of the model then has the form

$$\mathcal{H}_{tot} = \mathcal{H} + h(t) ,$$
$$\mathcal{H} = \sum_{n,m} \beta_{nm} a_n^\dagger a_m , \quad h(t) = \sum_{n,m} h_{nm}(t) a_n^\dagger a_m . \tag{A1}$$

Absorption and emission spectra for (A1) are evaluated from the spectral densities[27]

$$F_{\vec{k}}(\omega) = (2\pi)^{-1} \int_{-\infty}^{\infty} dt \, e^{i\omega t} \langle a_{\vec{k}}(t) a_{\vec{k}}^\dagger(0) \rangle , \tag{A2}$$

$$f_{\vec{k}}(\omega) = (2\pi)^{-1} \int_{-\infty}^{\infty} dt \, e^{i\omega t} \langle a_{\vec{k}}^\dagger(t) a_{\vec{k}}(0) \rangle , \tag{A3}$$

where $a_{\vec{k}} = N^{-1/2} \sum_n \exp(i\vec{k}\cdot\vec{R}_n) a_n$ (N is the total number of sites), and $\langle\rangle$ denotes averaging of the fluctuating part of (A1), for a no-exciton state in (A2) and for a one-exciton state in (A3). It is convenient to work in an extended zone scheme such that the Davydov branches of the exciton become unfolded into a single band. Then photons will couple to certain special exciton wave vectors, in addition to $\vec{k} = 0$. For these values of $\vec{k}$, (A2) and (A3) give the normalized absorption and emission spectra, respectively, provided the spectral frequency range is small compared with the average frequency. The spectrum for each special value of $\vec{k}$ is the spectrum of the appropriate Davydov component.

Using methods and notation given by Kubo,[17] one has

$$\hat{a}_{\vec{k}}(t) = \exp_T\left[-i \int_0^t \hat{h}(t')^\times dt' \right] a_{\vec{k}} , \tag{A4}$$

where for any operator A the circumflex denotes the interaction picture, $\hat{A}(t) \equiv e^{i\mathcal{H}t} A(t) e^{-i\mathcal{H}t}$, T denotes time ordering of each term in the expansion of the exponential, and the superscript $\times$ indicates that a commutation operation is to be performed, i.e., $A^\times B \equiv [A, B]$. The average of (A4) over the fluctuating part is obtained from

$$\langle \exp_T[-i \int_0^t \hat{h}(t')^\times dt'] \rangle$$
$$= \exp_T\left[-\tfrac{1}{2} \int_0^t dt_1 \int_0^t dt_2 \langle \hat{h}(t_1)^\times \hat{h}(t_2)^\times \rangle_c \right] , \tag{A5}$$

where the subscript c denotes a cumulant average. We have used the fundamental assumption of the model that any cumulant average of a product of more than two quantities $h_{nm}(t)$ vanishes [as does

the average of a single $h_{nm}(t)$, since it is defined as a fluctuation about an average]. With the aid of (1), we have

$$\int_0^t dt_1 \int_0^t dt_2 \langle \hat{h}(t_1) \hat{h}(t_2)^\times \rangle_c = 2 \operatorname{sgn}(t) \int_0^t dt_1 \hat{Q}(t_1) , \tag{A6}$$

where

$$Q \equiv \sum_{n,m} \gamma_{n-m} (a_n^\dagger a_m)^\times [a_n^\dagger a_m + (1 - \delta_{nm}) a_m^\dagger a_n]^\times ,$$

and where $\operatorname{sgn}(t) = 1$ for $t > 0$ and -1 for $t < 0$. Substituting (A6) into (A5) and then into (A4), we obtain expressions for the integrands of (A2) and (A3). These expressions are easily evaluated by considering their equations of motion,

$$(\partial/\partial t) \langle a_{\vec{k}}(t) a_{\vec{k}}^\dagger(0) \rangle$$
$$= (\partial/\partial t) \langle 0 | e^{-i\mathcal{H}t} \langle a_{\vec{k}}(t) \rangle e^{i\mathcal{H}t} a_{\vec{k}}^\dagger | 0 \rangle$$
$$= -i \langle [\mathcal{H}, a_{\vec{k}}(t)] a_{\vec{k}}^\dagger \rangle - \operatorname{sgn}(t) \langle [Q(t) a_{\vec{k}}(t)] a_{\vec{k}}^\dagger \rangle , \tag{A7}$$

where $|0\rangle$ is the no-exciton state. Since $Q a_{\vec{k}} = \sum_n \gamma_n a_{\vec{k}} = \Gamma a_{\vec{k}}$, and, from (A1), $\mathcal{H} = N^{-1} \sum_{\vec{k}} \epsilon_{\vec{k}} a_{\vec{k}}^\dagger a_{\vec{k}}$, where $\epsilon_{\vec{k}} \equiv N^{-1} \sum_{n,m} \beta_{nm} \exp(i\vec{k}\cdot\vec{R}_n)$, we have

$$(\partial/\partial t) \langle a_{\vec{k}}(t) a_{\vec{k}}^\dagger(0) \rangle$$
$$= -i\epsilon_{\vec{k}} \langle a_{\vec{k}}(t) a_{\vec{k}}^\dagger(0) \rangle - \operatorname{sgn}(t) \Gamma \langle a_{\vec{k}}(t) a_{\vec{k}}^\dagger(0) \rangle , \tag{A8}$$

which, using $\langle a_{\vec{k}}(0) a_{\vec{k}}^\dagger \rangle = 1$, has the solution

$$\langle a_{\vec{k}}(t) a_{\vec{k}}^\dagger(0) \rangle = e^{-i\epsilon_{\vec{k}}t - \Gamma|t|} , \tag{A9}$$

yielding the absorption spectrum

$$F_{\vec{k}}(\omega) = \frac{\Gamma/\pi}{(\omega - \epsilon_{\vec{k}})^2 + \Gamma^2} . \tag{A10}$$

The calculation of the emission spectrum follows identical steps, except that in place of the expectation value of the no-exciton state $|0\rangle$ the trace over one-exciton states must be used. The result is $f_{\vec{k}}(\omega) = F_{\vec{k}}(\omega)$ [Eq. (A10)]. Thus the spectra are Lorentzians of width Γ for all Davydov components, centered about the appropriate energy $\epsilon_{\vec{k}}$ of each component.

APPENDIX B: DIFFUSION TENSOR

The spatial Fourier transform of Eq. (2) is given by

$$(\partial/\partial t) g_{\vec{R}}(\vec{q}) = -i \sum_{\vec{R}'} \beta_{\vec{R} - \vec{R}'} g_{\vec{R}'}(\vec{q})(1 - e^{i\vec{q}\cdot(\vec{R}' - \vec{R})})$$
$$- 2\Gamma g_{\vec{R}}(\vec{q}) + 2\delta_{\vec{R}0} [\gamma(\vec{q}) - \gamma_0] g_0(\vec{q})$$
$$+ 2\gamma_{\vec{R}} e^{-i\vec{q}\cdot\vec{R}} g_{-\vec{R}}(\vec{q}) , \tag{B1}$$

where

$$g_{\vec{R}}(\vec{q}) \equiv \sum_{\vec{R}'} e^{i\vec{q}\cdot\vec{R}'} \rho_{\vec{R}' + \vec{R}, \vec{R}'} , \tag{B2}$$

$$\gamma(\vec{q}) \equiv \sum_{\vec{R}} e^{i\vec{q}\cdot\vec{R}} \gamma_{\vec{R}} , \tag{B3}$$

and where the Hamiltonian $\mathcal{H}$ in Eq. (2) has been expressed in terms of its matrix elements $\beta_{\vec{R}}$ connecting molecules separated by the lattice vector $\vec{R}$. For convenience, labels n and m in Eq. (2) have

been replaced by the explicit lattice vectors for which they stand.

We consider Eq. (B1) in the limit of large times and small wave vectors $\vec{q}$ appropriate for a possible applicability of a macroscopic diffusion equation. For $\vec{R} \neq 0$, the left-hand side of Eq. (B1) can be neglected after times such that the system is sufficiently close to a steady-state limit so that the rates of change are small compared to Γ (times large compared to the scattering time). For present purposes, it is sufficient to solve the resulting equation under conditions such that

$$|g_0(\vec{q})| \gg |g_{\vec{R}}(\vec{q})| \quad \text{for all } \vec{R} \neq 0 . \tag{B4}$$

One obtains, using $\gamma_{\vec{R}} = \gamma_{-\vec{R}}$ [see Eq. (1)],

$$g_{\vec{R}}(\vec{q}) = -\tfrac{1}{2} i \beta_{\vec{R}} (\Gamma + \gamma_{\vec{R}})^{-1} (1 - e^{-i\vec{q}\cdot\vec{R}}) g_0(\vec{q})$$
$$(\vec{R} \neq 0) , \tag{B5}$$

so that, in order to satisfy (B4), one must have

$$\beta_{\vec{R}} (\Gamma + \gamma_{\vec{R}})^{-1} |\sin\tfrac{1}{2}\vec{q}\cdot\vec{R}| \ll 1 , \tag{B6}$$

which will always be obeyed for sufficiently small $\vec{q}$. Equation (B6) is essentially the statement that the wavelength of the exciton density modulation to be considered must be large compared to a mean free path, since $\beta_{\vec{R}} R$ is a measure of the exciton velocity and $1/\Gamma$ of its scattering time. Substitution of (B5) into Eq. (B1) for $\vec{R} = 0$ yields for $g_0(\vec{q})$, the Fourier transform of the exciton density, the relation

$$(\partial/\partial t) g_0(\vec{q}) = -2[\Gamma - \gamma(\vec{q})] g_0(\vec{q}) - g_0(\vec{q})$$
$$\times \{\textstyle\sum \beta_{\vec{R}}^2 [1 - \cos(\vec{q}\cdot\vec{R})]/(\Gamma + \gamma_{\vec{R}})\} , \tag{B7}$$

which in the limit $\vec{q} \to 0$ approaches the diffusion equation

$$(\partial/\partial t) g_0(\vec{q}) = -\vec{q}\cdot\vec{D}\cdot\vec{q} g_0(\vec{q}) , \tag{B8}$$

with

$$\vec{D} = \textstyle\sum_{\vec{R}} \vec{R}\vec{R} [\gamma_{\vec{R}} + \tfrac{1}{2}\beta_{\vec{R}}^2/(\Gamma + \gamma_{\vec{R}})] . \tag{B9}$$

If (B6) is obeyed for all $\vec{q}$ up to the zone boundary, we have the special case of the hopping model, where the mean free path is small compared to a lattice spacing. In this case (B7) is valid for all $\vec{q}$ and may be transformed back to the hopping equation,

$$(\partial/\partial t)\rho_{\vec{R}\,\vec{R}} = \textstyle\sum_{\vec{R}'} \Psi(R - R')\rho_{\vec{R}'\vec{R}'}$$
$$-[\textstyle\sum_{\vec{R}'} \Psi(\vec{R}')]\rho_{\vec{R}\vec{R}} , \tag{B10}$$

where

$$\Psi(\vec{R}) = 2\gamma_{\vec{R}} + \beta_{\vec{R}}^2/(\Gamma + \gamma_{\vec{R}}) . \tag{B11}$$

APPENDIX C: ERROR ANALYSIS

We assume that the measured delayed-fluorescence excitation spectrum $\Phi(\omega)$ contains a noise $\delta\Phi(\omega)$ whose correlation function is given by

$$\langle \delta\Phi(\omega)\delta\Phi(\omega')\rangle = \epsilon^2 \xi \delta(\omega - \omega') . \tag{C1}$$

Relation (C1) is the continuum limit for measurements made in discrete channels (such as those of the CAT) at intervals ξ of the variable ω. The quantity ϵ is the rms amplitude of the noise in each channel, assumed to be uncorrelated between different channels, and the same in all channels (as observed).

With (C1), the mean-square error in the mean energy $\overline{\omega}$ given by Eq. (10) becomes

$$\langle (\delta\overline{\omega})^2 \rangle = \frac{\tfrac{1}{4}\epsilon^2 \xi \int d\omega\, \omega^2/\Phi(\omega)}{\{\int d\omega [\Phi(\omega)]^{1/2}\}^2} , \tag{C2}$$

where we have assumed $\delta\Phi(\omega) \ll \Phi(\omega)$ for all ω's of interest. This can usually be achieved in practice, even in the wings of the spectra, by reducing the amplitude of $\delta\Phi(\omega)$ by taking an average over several channels. Averaging over n channels reduces the rms noise by $n^{-1/2}$, but increases the effective channel width by n. The quantity $\epsilon^2 \xi$ in (C1) remains, however, invariant under this procedure, so that its value is determined by the rms noise in a single channel. Similarly, the mean-square error in the effective linewidth Γ given by Eq. (12) will be [we neglect the Boltzmann factors in (12) for simplicity[30]]

$$\langle (\delta\Gamma)^2 \rangle = \epsilon^2 \xi \Gamma^2 \left(\frac{\int d\omega/\Phi(\omega)}{\{\int d\omega [\Phi(\omega)]^{1/2}\}^2} \right.$$
$$\left. - 2\frac{\int d\omega [\Phi(\omega)]^{-1/2}}{\int d\omega [\Phi(\omega)]^{1/2} \int d\omega \Phi(\omega)} + \frac{\int d\omega}{[\int d\omega \Phi(\omega)]^2} \right) . \tag{C3}$$

For purposes of estimating the errors (C2) and (C3), it is sufficient to approximate the measured excitation spectra by squares of Lorentzians, truncated within the experimental range of frequencies. For simplicity, we assume that this range is symmetric about the maximum of the Lorentzian, extending by an amount η on each side of the maximum. That is,

$$\Phi(\omega) \approx \Phi(0)\Gamma^4/(\omega^2 + \Gamma^2)^2 \quad \text{for } |\omega| \leqslant |\eta| , \tag{C4}$$

where $\omega = 0$ has been chosen at the position of the peak, whose measured height is $\Phi(0)$. Evaluation of (C2) yields

$$\langle (\delta\overline{\omega})^2 \rangle = \frac{\epsilon^2 \xi}{4\Gamma^6 \pi^2 \Phi(0)^2} (\tfrac{2}{7}\eta^7 + \tfrac{4}{5}\eta^5\Gamma^2 + \tfrac{2}{3}\eta^3\Gamma^4) . \tag{C5}$$

In present experiments, the range η was large compared to the linewidth ($\eta \approx 5\Gamma$) and the last two terms in (C5) are negligible. One obtains

$$\langle (\delta\overline{\omega})^2 \rangle^{1/2} \approx \frac{\pi^{-1}(\tfrac{1}{14}\xi\eta)^{1/2}(\eta/\Gamma)^3\epsilon}{\Phi(0)} . \tag{C6}$$

Similarly, the error in Γ is given by

$$\langle (\delta\Gamma)^2 \rangle^{1/2} \approx \frac{(\tfrac{2}{5})^{1/2}\xi^{1/2}\eta^{5/2}\epsilon}{\pi\Gamma^2 \Phi(0)} . \tag{C7}$$

APPENDIX D: CORRELATION FUNCTION IN HOPPING MODEL

The equation of motion of the exciton density $\rho_{\vec{R}\vec{R}}(t)$ has in the hopping model the general form given in Eq. (B10). The spatial Fourier transform of this equation is

$$(\partial/\partial t)g(\vec{q}, t) = -f(\vec{q})g(\vec{q}, t) , \qquad (D1)$$

where

$$f(\vec{q}) \equiv \sum_{\vec{R}}(1 - e^{i\vec{q}\cdot\vec{R}})\Psi(\vec{R}) \qquad (D2)$$

and

$$g(\vec{q}, t) \equiv \sum_{\vec{R}} e^{i\vec{q}\cdot\vec{R}}\rho_{\vec{R}\vec{R}}(t) . \qquad (D3)$$

Equation (D1) is easily solved to yield $\rho_{00}(t)$ for the case corresponding to the initial condition $\rho_{\vec{R}\vec{R}}(0)$ $= \delta_{\vec{R}0}$. This $\rho_{00}(t)$ gives the probability that an exciton, which is at $\vec{R} = 0$ at time $t = 0$, is still at $\vec{R} = 0$ at time t. The real part of its Fourier transform with respect to time is the correlation function[41] $J(\omega)$ needed in the analysis of triplet-exciton-induced proton spin relaxation. The result is

$$J(\omega) = (N\pi)^{-1}\sum_{\vec{q}}f(\vec{q})/\{\omega^2 + [f(\vec{q})]^2\} . \qquad (D4)$$

For triplets in anthracene, the motion is nearly two dimensional and the important hopping rates are Ψ_d and Ψ_b for transfer between molecules separated by lattice vectors equivalent to $\frac{1}{2}(\vec{a} + \vec{b})$ and $\vec{b}$, respectively.[33-35] On appropriately replacing the wave-vector sum in (D4) by an integration, one obtains

$$J(\omega) = (ab/16\pi^3)\int_0^{4\pi/a} dq_a$$

$$\times \int_0^{4\pi/b} dq_b f(q_a, q_b)/\{\omega^2 + [f(q_a, q_b)]^2\} , \qquad (D5)$$

where

$$f(q_a, q_b) = 4\Psi_d + 2\Psi_b - 4\Psi_d \cos(\tfrac{1}{2}q_a a)\cos(\tfrac{1}{2}q_b b)$$

$$- 2\Psi_b \cos(q_b b) . \qquad (D6)$$

Expression (D5) diverges as $\omega \to 0$. As follows[46] from (D2) and (D4), such a divergence will occur whenever the motion is confined to one or two dimensions and is a manifestation of the exciton's repeated return to the origin in these cases.[45] The divergence of (D5) is not present in reality, because of the weak transfer perpendicular to the ab plane.[2,37] As shown in Ref. 37, such nearly two-dimensional motion can be approximated by a motion constrained to the ab plane but with an effective exciton decay rate equal to the out-of-plane hopping rate. This approximation here amounts to adding the out-of-plane hopping rate $\Psi_{c*} = 2\Psi_{c+d}$ to the right-hand side of (D6).

The evaluation of (D5) for purposes of Fig. 2 was performed by numerical integration. For curve A the room-temperatures values of Ψ_d and Ψ_b implied by the measured[2] values of D_{aa} and D_{bb} were used; for Ψ_{c*} the lower value deduced[37] from magnetic field experiments was used. Setting $\Psi_{c*} = 0$, however, does not significantly affect $J(\omega)$ for the frequency range shown in Fig. 2. Curve B gives the corresponding behavior for a fivefold increase in the hopping rates Ψ_d and Ψ_b. The Lorentzian approximation used in Refs. 8 and 9 results if $f(q_a, q_b)$ in (D5) is replaced by its average value $\Psi_{tot} = 4\Psi_d$ $+ 2\Psi_b$. The correlation function reduces then to $J(\omega) = \pi^{-1}\Psi_{tot}/(\omega^2 + \Psi_{tot}^2)$. As illustrated in Fig. 2, the Lorentzian correlation function (dashed curve) becomes a reasonable approximation in the vicinity of magnetic fields for which $\omega \approx \Psi_{tot}$, the reciprocal of the total residence time.[44]

*Present address: Facultad de Ingenieria, Departamento de Fisica, Paseo Colón 850, Buenos Aires, Argentina.

†Contribution No. 1853.

[1] For references prior to 1968, see the review article by P. Avakian and R. E. Merrifield, Mol. Cryst. 5, 37 (1968).

[2] V. Ern, Phys. Rev. Letters 22, 343 (1969).

[3] D. C. Hoesterey and G. W. Robinson, J. Chem. Phys. 54, 1709 (1971); M. Drew and D. F. Williams, ibid. 54, 1844 (1971).

[4] P. Avakian, V. Ern, R. E. Merrifield, and A. Suna, Phys. Rev. 165, 974 (1968).

[5] G. Durocher and D. F. Williams, J. Chem. Phys. 51, 1675 (1969).

[6] G. A. George and G. C. Morris, Mol. Cryst. Liquid Cryst. 10, 115 (1970); S. Arnold, W. B. Whitten, and A. C. Damask, Phys. Rev. B 3, 3452 (1971).

[7] D. Haarer and H. C. Wolf, Mol. Cryst. Liquid Cryst. 10, 359 (1970).

[8] G. Maier, U. Haeberlen, and H. C. Wolf, Phys. Letters 25A, 323 (1967).

[9] H. Kolb and H. C. Wolf, Z. Naturforsch. (to be published).

[10] D. H. Goode and D. F. Williams, in Proceedings of the Fifth Molecular Crystal Symposium, Philadelphia, 1970 (unpublished); and unpublished.

[11] H. Haken and G. Strobl, in The Triplet State, edited by A. B. Zahlan (Cambridge U.P., Cambridge, England, 1967), pp. 311–314.

[12] M. Grover and R. Silbey, J. Chem. Phys. 54, 4843 (1971).

[13] H. Haken and P. Reineker, in Excitons, Magnons and Phonons in Molecular Crystals, edited by A. B. Zahlan (Cambridge U.P., Cambridge, England, 1968), pp. 185–194.

[14] D. L. Dexter, J. Chem. Phys. 21, 836 (1953).

[15] M. Trlifaj, Czech. J. Phys. 6, 533 (1956).

[16] R. E. Merrifield, J. Chem. Phys. 48, 3693 (1968).

[17] R. Kubo, J. Phys. Soc. Japan 17, 1100 (1962).

[18] W. A. Bingel, Can. J. Phys. 37, 680 (1959).

[19] R. Kubo, J. Phys. Soc. Japan 12, 588 (1957).

[20] It is worthwhile to dispel a potential source of confusion created by statements in Refs. 11 and 13 to the effect

that, for a one-dimensional system with nearest-neighbor interactions and local scattering, diffusive motion is absent whenever the scattering rate Γ is less than the exciton bandwidth. A closer examination of this problem shows that, for the stated condition, coherent exciton motion takes place over an extended (but finite) region in space; i.e., the exciton motion can no longer be thought of as a random walk or intramolecular hopping process. On a macroscopic scale the motion is, of course, diffusive for arbitrarily small (but nonzero) Γ.

[21]J. Jortner, S. Choi, J. L. Katz, and S. A. Rice, Phys. Rev. Letters 11, 323 (1963).

[22]A factor ω^{-4} in the original formula has been replaced by a constant, since the relative variation of ω over the range of interest is very small.

[23]G. J. Sloan, Mol. Cryst. 1, 161 (1966).

[24]S. Arnold, W. B. Whitten, and A. C. Damask, J. Chem. Phys. 53, 2878 (1970).

[25]R. M. Hochstrasser, J. Chem. Phys. 47, 1015 (1967).

[26]I. Nakada, J. Phys. Soc. Japan 20, 346 (1965).

[27]A. Suna, Phys. Rev. 135, A111 (1964).

[28]D. F. Williams, J. Chem. Phys. 47, 344 (1967); H. P. Müller, P. Thoma, and G. Vaubel, Phys. Status Solidi 23, 253 (1967); G. C. Smith, Phys. Rev. 166, 839 (1968).

[29]The low-resolution phosphorescence emission spectra were recorded with a technique similar to that used for the absorption experiments. The triplets were generated by intersystem crossing from the singlet manifold excited by strongly absorbed blue and near-uv light (1000-W xenon arc lamp filtered through 10 cm of water and Corning C.S. 5-56 plus heat-absorbing Jaegers No. 3029 and Schott KG-3 filters). The temperature of the crystals was lowered with a small glass cryostat with optical (Suprasil No. 1) front and rear windows. The cryostat was placed between the two blades of a phosphoroscope (rotating at 1800 rpm) with $\frac{1}{2}$ and $\frac{1}{4}$ cutout sectors for the front and the rear blade, respectively. The emission was detected with a cooled (to 0 °C with EMI cooler model ZD-50) photomultiplier (EMI 9558QA) through a Corning C.S. 2-59 filter and the Spex monochromator described above set for a 16-Å resolution. Only measurements on freshly cleaved crystals were considered reliable, since prolonged excitation (several hours) resulted in broadening of the emission lines.

[30]When the range of $\hbar\omega$ is small compared to kT, one can neglect the Boltzmann factors in this formula; in the present calculations, such a neglect would have introduced an error in Γ of about 5%.

[31]Only local densities of states are involved in the theory of Ref. 15, and absorption or emission spectra must be insensitive to the relative phase of the wave function on different molecules.

[32]The structure in the a-polarized spectrum, indicating a shoulder displaced to lower energies by about 40 cm^{-1} from the main peak, is possibly a hot band due to coupling of the exciton to the lowest optical phonon in anthracene [see G. S. Pawley, Phys. Status Solidi 20, 347 (1967)]. This phonon has about the right energy and the right symmetry for the optical observation of this phonon to-

gether with the "plus" Davydov component of the exciton. The other Davydov branch of this phonon, which should couple about equally strongly to the "minus" exciton, appears to be an acoustic branch, with zero energy at $\tilde{k}=0$. This circumstance would explain the weakness of the shoulder at the corresponding position in the b-polarized spectrum.

[33]M. Levine, J. Jortner, and A. Szöke, J. Chem. Phys. 45, 1591 (1966); S. A. Rice and J. Jortner, in Physics of Solids at High Pressures, edited by C. T. Tomizuka and R. M. Emrick (Academic, New York, 1965), pp. 63–168; J. Jortner, S. A. Rice, J. L. Katz, and S. Choi, J. Chem. Phys. 42, 309 (1965).

[34]C. E. Swenberg, J. Chem. Phys. 51, 1753 (1969).

[35]A. Tiberghien and G. Delacôte, J. Phys.(Paris) 31, 637 (1970).

[36]Calculated values of the β's can be used to obtain estimates of the fluctuation rates γ_a, γ_b, and γ_{a+c}, if the principal components of the diffusion tensor are known. As an example, with the β's of Ref. 35 (which presently have the best over-all agreement with observed Davydov splittings for both anthracene and naphthalene), using the tensor components of Ref. 2 and the value of $\gamma=51$ cm^{-1} from present experiments, one obtains for anthracene at room temperature $\gamma_a=7\times10^{-2}$ cm^{-1}, $\gamma_b=2\times10^{-2}$ cm^{-1}, and $\gamma_{a+c}=2\times10^{-3}$ cm^{-1}, where a Franck-Condon factor of $\frac{1}{4}$ has been assumed for the 0, 0 peak. If, instead, the lower value for D_{c*c*} deduced (Ref. 37) from magnetic field experiments is used, the estimate of γ_{a+c} is reduced to 0.3×10^{-3} cm^{-1}.

[37]A. Suna, Phys. Rev. B 1, 1716 (1970).

[38]A. McL. Mathieson, J. M. Robertson, and V. C. Sinclair, Acta Cryst. 3, 245 (1950); 3, 251 (1950).

[39]A more stringent upper limit on γ_a can be obtained from the measured value of D_{aa} by neglecting β_a in (13a).

[40]H. Sternlicht and H. M. McConnell, J. Chem. Phys. 35, 1793 (1961).

[41]A. Abragam, The Principles of Nuclear Magnetism (Oxford U.P., New York, 1961), Chaps. 8–10.

[42]Although this spin Hamiltonian arises from the dipolar interaction between the electron and hole comprising the exciton, the fluctuations in this latter interaction due to the exciton's motion give a negligible contribution to spin relaxation, since the motion of both electron and hole in their respective orbitals is extremely rapid compared to exciton hopping rates. The authors are indebted to Professor D. J. Scalapino for a discussion of this point.

[43]G. Maier, U. Haeberlen, H. C. Wolf, and K. H. Hausser, Phys. Letters 25A, 384 (1967).

[44]This diffusion constant leads to an exciton residence time (see Appendix D) equal to about 4.5×10^{-12} sec. The field for which the exciton spin precession period equals this residence time is about 12 kOe.

[45]See, for example, W. Feller, An Introduction to Probability Theory and Its Applications (Wiley, New York, 1957), Vol. I, p. 327.

[46]For $\Psi(\tilde{R})=\Psi(-\tilde{R})$, Eq. (D2) predicts $f(\tilde{q})\sim q^2$ for small q. The continuum limit of (D4) in n dimensions leads to an integral whose integrand, for $\omega=0$ and small q, varies as $q^{n-1}/f(\tilde{q})\sim q^{n-3}$, so that a divergence results for $n<3$.